DOI: 10.26599/FSHW.2026.9250957

Contents lists available at SciOpen

Food Science and Human Wellness

journal homepage: https://www.sciopen.com/journal/2097-0765

China Food Publishing Co.

Alistipes indistinctus with potential probiotic characteristics prevents lipopolysaccharide-induced intestinal barrier injury

Yingxi Xu[1, #], Ludi Liu[1, #], Tianyi Wang[2], Huanshuai Yang[3], Siping Liao[3], Shanshan Zhu[3], Jiangyuan Zhu[3], Yawen Zhao[3], Min Xia[3], Yan Liu[3,*]

[1]*Guangdong Provincial Key Laboratory of Food, Nutrition and Health, Department of Statistics and Epidemiology, School of Public Health, Sun Yat-sen University, Guangzhou, Guangdong, 510080, China*

[2]*Department of Nutrition and Food Hygiene, School of Public Health, Guilin Medical University, Guilin, Guangxi, 541199, China*

[3]*Guangdong Provincial Key Laboratory of Food, Nutrition and Health, Department of Nutrition, School of Public Health, Sun Yat-sen University, Guangzhou, Guangdong, 510080, China*

ABSTRACT: Gut barrier integrity is indispensable for health and has been recognized as a key mechanism through which probiotics exert their beneficial effects. Recently, *Alistipes indistinctus* (*A. indistinctus*) has attracted increasing interest due to its pleiotropic benefits on metabolic homeostasis. However, evidence supporting its probiotic properties remains limited. Here, genomic analysis followed by a series of *in vitro* and *in vivo* studies was performed to systematically evaluate the safety, gastrointestinal tolerance, adhesive capacity, and intestinal barrier protection effect of *A. indistinctus*. *A. indistinctus* exhibited a high genomic sequence similarity with *Bifidobacterium spp*., an established probiotic, and encoded a variety of genes related to antioxidation and bile salt hydrolysis. The survival rate of *A. indistinctus* in gastric and intestinal fluid was 77.3% and 73.0%, respectively, comparable to most well-known probiotics. Transmission electron microscopy analysis further demonstrated that only live *A. indistinctus* exhibited a high adherence capacity to intestinal villi, which facilitated its colonization. Consistently, oral administration of live *A. indistinctus* led to a 1.5-fold increase in the number of goblet cells, which in turn boosted the formation and thickness of mucus layer in germ-free mice, and enhanced the expression of tight junctions, with no sign of liver and renal injury. Similarly, co-culture with *A. indistinctus* substantially reversed the impaired expression of mucin 2 in LS174T and zonula occludens-1 and occludin in Caco-2 cells, induced by lipopolysaccharide exposure. Mechanistically, *A. indistinctus* enhanced gut integrity and protected against lipopolysaccharide-induced inflammation by suppressing the nuclear translocation and activation of nuclear factor kappa-B p65 in both goblet and epithelial cells. Collectively, our findings provide a mechanistic basis for the protective effects of *A. indistinctus* on intestinal barrier integrity, highlighting its potential as a next-generation probiotic.

Keywords: *Alistipes indistinctus*; probiotics; intestinal barrier; anti-inflammation; intestinal colonization

1. Introduction

The integrity of intestinal barrier consists of a variety of mucosal structural components and molecules[1]. The first line of defense is the mucus layer, a gel-like sieve of glycosylated mucins, which contains immune regulators like antimicrobial peptides and secretory IgA to enhance barrier function[2, 3]. Underneath the

[#]These authors contributed equally to this work
***Corresponding author**
liuyan215@mail.sysu.edu.cn (Y. L.)

Received 29 July 2025
Received in revised from 26 August 2025
Accepted 13 October 2025

mucus layer, the intestinal epithelial cells form a continuous monolayer interconnected by junctional complexes, constituting a physical barrier[4]. Defects of intestinal barrier have been associated with various disorders, such as inflammatory bowel disease, obesity, diabetes, and fatty liver disease[5]. Thus, restoring intestinal barrier has been regarded as a promising approach for the management of metabolic disorders.

Probiotics are a group of active microorganisms which can colonize in the gastrointestinal tract and confer health benefits to the host[6], partially through a modulation of intestinal integrity[7]. Recently, *Alistipes indistinctus* (*A. indistinctus*), an anaerobic, gram-negative bacterium, has emerged as a promising candidate for next-generation probiotics. Initially isolated from healthy infant feces, *A. indistinctus* is a common symbiotic microbe without harmful metabolites[8], colonizing in approximately 52%–69% of healthy individuals[9]. As a keystone bacterium, *A. indistinctus*, together with seven other probiotics, such as *Porphyromonas loveana* and *Dialister pneumosintes*, was capable of restoring the microbial composition of the nonalcoholic fatty liver disease toward a normal gut microbiome with 92.3% recovery[10]. Furthermore, a large-scale metagenomic analysis identified *A. indistinctus* as the bacterium showing the strongest negative association with both ulcerative colitis and Crohn's disease[11]. More importantly, beyond observational evidence, the beneficial effects of *A. indistinctus* have been documented in experimental studies. For instance, *A. indistinctus* was found to improve glucose intolerance by enhancing the degradation of complex monosaccharides, thereby increasing energy harvest and metabolic efficiency in high fat diet-induced obesity[12]. Moreover, gavage of *A. indistinctus* attenuated the risk of hyperuricemia via enhancing intestinal uric acid excretion[13]. Collectively, these findings underscore *A. indistinctus* as a critical regulator of intestinal health and metabolic homeostasis. However, despite growing evidence regarding its metabolic benefits, it remains unclear whether *A. indistinctus* fulfills the criteria for probiotics proposed by the International Scientific Association for Probiotics and Prebiotics (ISAPP)[14], which hinders its application as a next-generation probiotics.

To address this knowledge gap, we investigated the probiotic properties of *A. indistinctus* using both germ-free mice and cell lines.

2. Materials and methods

2.1 Comparative genomic analysis

The genomic sequences for *A. indistinctus* (*Alistipes indistinctus* YIT 12060) and two established probiotic bacteria, *Bifidobacterium* spp. and *Lactobacillus* spp., were downloaded from the NCBI (https://www.ncbi.nlm.nih.gov/) references sequence database for comparative genomic analysis. The alignment and identification of homologous regions were performed using the ProgressiveMauve software, which utilized a progressive alignment algorithm to detect conserved sequences while accounting for genomic rearrangements, inversions, and insertions. The alignment was conducted under default settings, including a minimum locally collinear block (LCB) weight threshold and an optimized seed weight, to ensure an accurate identification of syntenic and homologous regions across the genomes. Moreover, genes related to probiotic

characteristics were downloaded from the UniProt database and compared against the genome of *Alistipes indistinctus* YIT 12060 to determine its probiotic characteristics at the genetic level.

2.2 In vivo experiments

2.2.1 Animal model

All animal experiments were performed in accordance with the Guidelines for Care and Use of Laboratory Animals of the Sun Yat-sen University and approved by the Animal Ethics Committee of the Sun Yat-sen University (No. 2024000544). Eight-week male mice on C57BL/6J background were obtained from Shenzhen Jingtuo Biotechnology Co., Ltd and housed under germ-free (GF) conditions or purchased from Vital River Laboratory Animal Technology (Beijing, China) and housed in SPF conditions at Sun Yat-sen University. All the animals were kept in groups of five mice per cage, with free access to food and water under a strict 12-h light/dark cycle at a controlled temperature (23±2°C).

GF mice were randomly divided into three groups and treated with 200 μL of sterile phosphate-buffered saline (PBS group), live *A. indistinctus* (LAI group, 5×10^8 colony-forming units (cfu) per 200 μL) and heat-killed *A. indistinctus* (HKAI group, 5×10^8 cfu per 200 μL)[13, 15], respectively via oral gavage on a daily basis for 4 weeks. Serum levels of aspartate aminotransferase (AST), alanine aminotransferase (ALT), creatinine, and blood urea nitrogen (BUN) were quantified using commercial kits (AST, C010-2-1; ALT, C009-2-1; Creatinine, C011-2-1; BUN, C013-1-1; Nanjing Jiancheng Bioengineering Institute, China).

For *A. indistinctus* colonization, SPF mice were gavaged with live *A. indistinctus* (5×10^8 cfu per 200 μL) daily for one week. After the cessation of gavage, fecal samples were collected at a fixed time every morning for another 7 days to evaluate the colonization capacity of *A. indistinctus*. Genomic DNA was isolated from fecal samples and colonic mucosal tissues using the MagMAX Microbiome Ultra Nucleic Acid Isolation Kit (A42358, Thermo Fisher Scientific, USA) following the manufacturer's protocols. DNA concentrations were quantified using an Infinite M200 Pro microplate reader (Tecan Group Ltd., Switzerland). For quantitative PCR (qPCR) analysis, template inputs were standardized at 40 ng (fecal DNA) or 80 ng (mucosal DNA). Target-specific primer sequences for *A. indistinctus* and universal bacterial amplification are detailed in **Table S1**.

2.2.2 Histological analysis

Liver and kidney were fixed with 4% paraformaldehyde, embedded in paraffin, and sectioned and stained with hematoxylin and eosin (H&E) for histological evaluation and inflammation assessment. Proximal colon segments were immediately removed and fixed for 24 h at room temperature in Carnoy's solution (G1120, Servicebio, China) and embedded in paraffin. Serial sections (5 μm) were prepared from the paraffin blocks, mounted onto glass slides, and stained with either H&E or Alcian Blue-Periodic Acid Schiff (AB-PAS).

2.2.3 Immunofluorescence staining and quantification

Following deparaffinization and antigen retrieval (G1202, Servicebio), paraffin-embedded samples, including distal colon tissues and cell lines, were permeabilized with 0.5% Triton X-100 for 10 min and

blocked with 10% goat serum for 10 min at room temperature. Specimens were then incubated overnight at 4°C with primary antibodies, including zonula occludens-1 (ZO-1, 21773-1-AP, Proteintech, China), occludin (OCLN, 27260-1-AP, Proteintech, China), and mucin 2 (MUC2, 27675-1-AP, Proteintech, China), followed by an incubation with corresponding fluorescent secondary antibodies for another 2h at room temperature in darkness. Nuclei were counterstained with 4',6-diamidino-2-phenylindole (DAPI; C1002, Beyotime Biotechnology, China). Fluorescence images were acquired using a Zeiss LSM 900 confocal microscope and analyzed with ZEN imaging software (Carl Zeiss AG, Germany) and ImageJ (National Institutes of Health, USA).

2.2.4 Reverse transcription and real-time PCR

Total RNA was isolated from tissue samples and cells using TRIzol reagent (15596026CN, Thermo Fisher Scientific, USA). For each sample, 500 ng of total RNA underwent reverse transcription into complementary DNA (cDNA) utilizing the HiScript III All-in-one RT SuperMix Kit (R333-01, Vazyme Biotech Co., Ltd, China). Quantitative real-time PCR (qPCR) analysis was subsequently performed on a QuantStudio 6 Pro Real-Time PCR System (Applied Biosystems, USA) with Taq Pro Universal SYBR qPCR Master Mix (Q712, Vazyme Biotech Co., Ltd, China). Primer sequences used in this study were provided in **Table S1**.

2.2.5 Western blotting

Total protein (30 μg per sample) was resolved by 10% SDS-PAGE and subsequently transferred to polyvinylidene fluoride membranes (ISEQ00010, Merck Millipore, USA). The membranes were blocked for 2h at ambient temperature with 5% (w/v) milk in Tris-buffered saline containing Tween-20 (TBST). Following blocking, membranes were incubated overnight at 4°C with primary antibodies, including ZO-1, OCLN, MUC2, NF-κB p65 (8242S, Cell Signaling Technology, USA), and phosphorylated NF-κB p65 (p-NF-κB p65; 3033S, Cell Signaling Technology). Following primary antibody incubation, membranes were probed for 1.5h at room temperature with appropriate horseradish peroxidase (HRP)-conjugated secondary antibodies. Specific bands were visualized using an enhanced chemiluminescence (ECL) detection kit (34580, Thermo Fisher Scientific, USA).

2.3 In vitro experiments

2.3.1 Bacterial strains, cells and culture conditions

A. indistinctus was obtained from DSMZ-German Collection of Microorganisms and maintained at 37°C for 48h in peptone-yeast extract-glucose (PYG) medium under anaerobic conditions (Bactron EZ-2, shellab, USA). Absorbance at 600 nm was measured using a microplate reader to determine its concentration. The bacterial cells of *A. indistinctus* were pelleted via centrifugation at 3,000 rpm at 4℃ for 5 min, followed by washing and resuspension in sterile reduced PBS buffer to achieve a final concentration of 5×10^8 cfu per 200 μL. *A. indistinctus* was inactivated by pasteurization for 30 min at 70℃, as previously described[16]. The bacterial suspensions were prepared freshly for animal experiments. Prior to use, the identity and purity of the

A. indistinctus culture were confirmed by sequencing and subsequent alignment to type strains using the Basic Local Alignment Search Tool (BLAST).

LS174T and Caco-2 cells were obtained from American Type Culture Collection, and were cultured in Minimum Essential Medium (MEM, C11095500BT, Gibco, USA) supplemented with 1% penicillin-streptomycin and 10% fetal bovine serum (FBS), and MEM supplemented with 1% penicillin-streptomycin and 20% FBS, respectively. Cells were incubated at 37°C in a humidified atmosphere containing 5% CO_2.

2.3.2 Transit tolerance against simulated gastrointestinal juices

Tolerance to gastrointestinal conditions was assessed using simulated digestive juices (composition detailed in **Table S2**). All juices were filtered with 0.22 μm membrane for sterilization prior to use. *A. indistinctus* was inoculated into 1 mL simulated gastric fluid and incubated anaerobically at 37°C for 2h. Gastric survival was determined by viable counts on PYG agar following incubation. For intestinal phase simulation, 0.5 mL duodenal solution and 0.5 mL bile solution were added to gastric-digested samples, followed by anaerobic incubation at 37°C for additional 2h. Gastrointestinal tolerance was quantified via colony-forming units.

2.3.3 BSH activity determination

BSH activity was assessed as previously described[17]. Briefly, 10 μL suspensions with 2×10^9 cfu of *A. indistinctus* were spot inoculated on a dry surface of Columbia blood agar supplemented with 5 g/L bile salts and incubated at 37°C for 72 h. Positive BSH activity was recorded when a white precipitate was found.

2.3.4 Cell Viability Assay

Cell viability was evaluated using the Cell Counting Kit-8 (CCK-8; Apexbio, USA) according to the manufacturer's instructions. Briefly, Caco-2 and LS174T cells were seeded in 96-well plates at a density of 1×10^4 cells per well and cultured for 24h. The cells were then treated with *A. indistinctus* at concentrations ranging from 0.6 OD to 2.4OD for 24h. PBS-treated cells were used as control. After treatment, supernatant was aspirated and the cells were washed once with sterile PBS, followed by the addition of MEM. 10 μL of CCK-8 reagent was added to each well and incubated for 2h at 37°C. The absorbance was measured at 450 nm using a microplate reader. Cell viability was calculated as follows:

$$\text{Cell Viability (\%)} = \frac{\text{Abs}_{\text{sample}} - \text{Abs}_{\text{blank}}}{\text{Abs}_{\text{control}} - \text{Abs}_{\text{blank}}} \times 100$$

where $\text{Abs}_{\text{sample}}$, $\text{Abs}_{\text{control}}$ and $\text{Abs}_{\text{blank}}$ represented the absorbance of *A. indistinctus*-treated groups, PBS-treated control group, and cell-free background control, respectively.

2.3.5 Detection of inflammatory cytokines

LS174T and Caco-2 cells were seeded in 12-well plates and treated *A. indistinctus* at 1.0×10^8 cfu/mL for 1h, followed by stimulation with 1 μg/mL E. coli O55:B5 lipopolysaccharide (LPS; L2880, Sigma-Aldrich, USA) for another 24h . Supernatants were collected and analyzed for secreted cytokines using commercial ELISA kits, including tumor necrosis factor-alpha (TNF-α; MM-0122H1), interleukin-1β (IL-1β;

MM-0181H1), and interleukin-6 (IL-6; MM-0049H1), which were obtained from Jiangsu Meimian Industrial Co., Ltd.

2.3.6 Intestinal epithelial barrier function assay

The trans-epithelial electrical resistance (TEER) measurements were conducted according to an established protocol[18] with minor modifications. Briefly, Caco-2 cells were seeded onto Transwell inserts (14212-1, LABSELECT) at 3×10^5 cells/mL and cultured for 18 days at 37°C to establish differentiated intestinal monolayers. TEER values were quantified using a Millicell ERS-2 volt-ohm meter (MERS00002, MilliporeSigma, USA). Monolayers demonstrating mean TEER values ≥400 Ω·cm² (triplicate measurements) were utilized for subsequent experiments. Qualified monolayers were pre-treated with *A. indistinctus* (1.0×10^8 cfu/mL) for 1h, followed by stimulation with 100 μg/mL LPS for another 24h before subjected to analysis.

The paracellular permeability assay was assessed via fluorescein isothiocyanate-dextran 4 kDa (FITC-dextran 4; FD-4, Sigma-Aldrich) flux as previously described[19]. Following PBS washes for two times, treated monolayers received 0.5 mL pre-heated Phenol Red Free MEM medium (51200038, Gibco) containing 1 mg/mL FD-4 in the apical chamber. After 2h, 100 μL basolateral medium was collected, and fluorescence intensity was measured at excitation/emission wavelengths of 492/520 nm to quantify paracellular flux.

2.3.7 Transmission electron microscopy

Caco-2 cells were seeded in 6-well plates at a density of 1.0×10^6 cells/mL and exposed to *A. indistinctus* (1.0×10^8 cfu/mL) for 1h. After treatment, cells were fixed with 2.5% glutaraldehyde followed by 1% osmium tetroxide post-fixation. Samples underwent dehydration through an ascending ethanol series and propylene oxide treatment, then embedded in resin. Ultrathin sections (50 nm) were prepared and contrasted with 3% uranyl acetate and lead citrate. Imaging was performed using a Philips CM100 transmission electron microscope.

2.4 Statistical analyses

Data were presented as mean ± standard error of mean (SEM), and all the analyses were performed by GraphPad Prism 9.0. Comparison between groups were performed using one-way ANOVA followed by Tukey's multiple comparison tests. Two-sided $P < 0.05$ was considered statistically significant.

3. Results

3.1 Genome properties of A. indistinctus

To investigate the probiotic properties and potential of *A. indistinctus*, we compared the whole genome reference sequence of *A. indistinctus* YIT 12060 with those of two common probiotic bacteria. Collinearity analysis revealed substantial homologous and collinear regions between strain *A. indistinctus* and *Bifidobacterium* spp., as well as between *A. indistinctus* and *Lactobacillus* spp. (**Figure 1**). Notably, the number of homologous and collinear regions was significantly higher between *A. indistinctus* and *Bifidobacterium* spp. than between *A. indistinctus* and *Lactobacillus* spp., suggesting that the probiotic

properties of *A. indistinctus* might resemble those of *Bifidobacterium* spp.. Specifically, the shared genomic regions between *A. indistinctus* and *Bifidobacterium* spp. harbored the *tuf* gene encoding elongation factor Tu (EF-Tu), which was responsible for the adhesion to intestinal epithelium and suppression of LPS- and pathogen-induced apoptosis[20]. Similarly, the conserved regions also contained the *groL* gene, which encoded the chaperonin GroEL protein, a well-known anti-inflammatory protein of established probiotics[21]. Comparative genomics analysis further demonstrated that *A. indistinctus* was able to encode mucus-binding proteins (MUBs), a class of effector molecules involved in the adhesion of *Lactobacillus* spp. to the host[22, 23]. Additionally, the genome of *A. indistinctus* also contained genes of Na^+/H^+ antiporter protein, antioxidant enzymes, bile salt hydrolytic (BSH) enzyme and carbohydrate-active enzymes synthase (**Table 1**), which were closely associated with the classical probiotic properties such as digestive tolerance and short-chain fatty acids production[24, 25]. Collectively, the genomic characteristics indicated a strong probiotic potential of *A. indistinctus*.

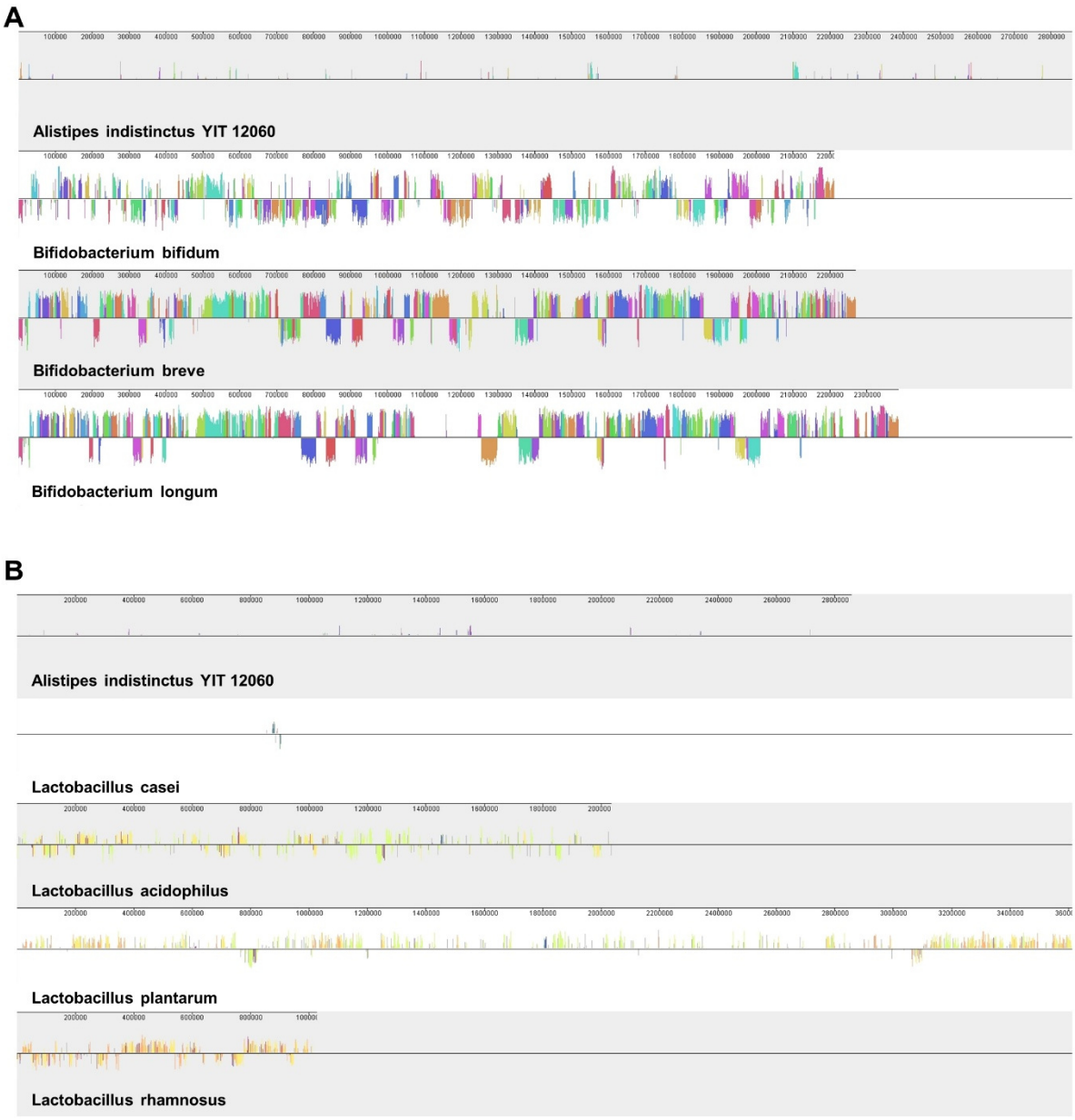

Figure 1. Genome characteristics of *A. indistinctus*. (A) Collinearity analysis of *A. indistinctus* with 3 reference strains of *Bifidobacterium* spp.. (B) Collinearity analysis of *A. indistinctus* with 4 reference strains of *Lactobacillus* spp..

Table 1 Encoding gene locus related to probiotic characteristics in the genome of *A. indistinctus*.

Protein name	Encoding gene locus
Na+/H+-antiporter	NQ495_RS05095
	NQ495_RS10810
	NQ495_RS02880
Bile salt hydrolytic enzyme	NQ495_RS03255
	NQ495_RS06775
Mucus-binding protein	NQ495_RS03110
Carbohydrate-Active Enzymes	NQ495_RS09515
	NQ495_RS00050
	NQ495_RS03060
	NQ495_RS05960
Antioxidant Enzymes	NQ495_RS05605
	NQ495_RS04720

3.2 The safety and colonization capacity of A. indistinctus

3.2.1 The safety of A. indistinctus

Given that the health-promoting effects of *A. indistinctus* depended on its viability[13], we first assessed its safety *in vivo*. Histological analysis revealed no pathological changes or inflammatory infiltration in either liver or kidney in mice gavaged with live *A. indistinctus* (**Figure 2A**). Moreover, no obvious difference in common indicators of hepatic and renal injuries, such as AST, serum creatinine, and urea nitrogen, was found in mice administered with live *A. indistinctus* compared to PBS control. However, serum ALT was almost halved in mice gavaged with live *A. indistinctus* (**Figure 2B-2E**), suggesting a favorable liver and kidney safety. Similarly, a negligible effect on cell viability was found in LS174T and Caco-2 cells exposed to an increasing dose of viable *A. indistinctus* (**Figure 2F and 2G**), lending further support to the safety of *A. indistinctus*.

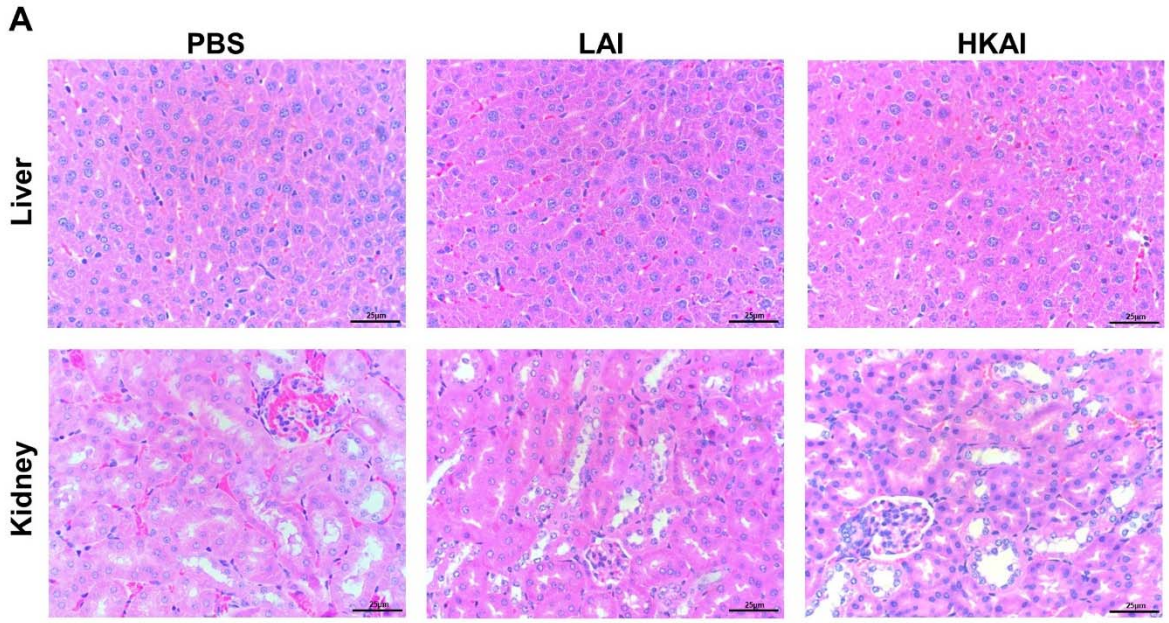

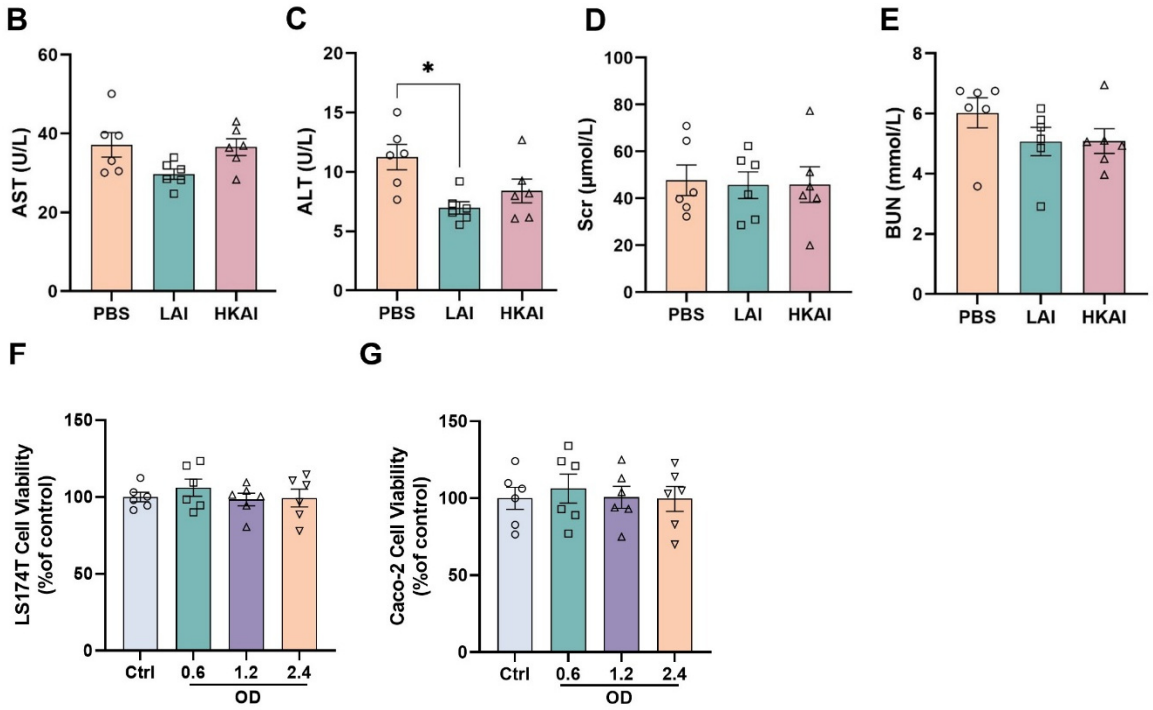

Figure 2. *A. indistinctus* had minimal hepatotoxicity and nephrotoxicity. (A) Representative H&E staining of liver and kidney (Scale bars, 25 μm). (B) Aspartate aminotransferase, (C) alanine aminotransferase activity, (D) creatinine, and (E) blood urea nitrogen level. Cell viability in (F) LS174T cells and (G) Caco-2 cells. Data were presented as mean ± SEM (n=6 per group for A-E, and n=6 independent experiments for F and G), and *P* values were determined by one-way ANOVA followed by Tukey's test. $^{*}P < 0.05$, $^{**}P < 0.01$, and $^{***}P < 0.001$.

3.2.2 The gastrointestinal transit tolerance and colonization capability of A. indistinctus

Furthermore, the gastrointestinal transit tolerance and colonization capacity of *A. indistinctus* was examined to evaluate its probiotic potential. As a strictly anaerobic microorganism, *A. indistinctus* exhibited a relatively slow growth rate, reaching the stationary phase after 36h (**Figure 3A**). After 2h of incubation, *A. indistinctus* showed strong resistance to both gastric and intestinal fluids, as evidenced by a survival rate of 77.3% and 73.0% in gastric and intestinal fluids, respectively. However, after an incubation in simulated gastric intestinal juices for 4h, the viable count of *A. indistinctus* was reduced from 1.0×10^{9} cfu/mL to 5.67×10^{8} cfu/mL (**Figure 3B**). Of note, such a survival rate was comparable to that observed in well-known probiotics, such as the *Bifidobacterium dentium* strain[19], suggesting a high gastrointestinal transit tolerance. In support of this observation, a variety of genes related to BSH activity, a key enzyme contributing to the survival and stability of probiotics in the gastrointestinal tract[26], could be encoded by the genome of *A. indistinctus* (**Figure 3C and Table S3**). Consistent with the functional inference, distinct white precipitated circles on blood plates with 0.5% bile acids was found with live *A. indistinctus* inoculation (**Figure. 3D**), further confirming its BSH activity. In line with its high gastrointestinal transit tolerance, live *A. indistinctus* could be successfully colonized in the intestine (**Figure. 3E**) and maintained a substantially higher abundance in the fecal samples compared to PBS control for at least one week after the cessation of gavage (**Figure. 3F**), indicating a strong adhesion capacity of live *A. indistinctus*. Consistently, transmission electron microscopy analysis revealed that live *A. indistinctus* adhered to the villi, which was absent in heat-killed *A. indistinctus*

(**Figure. 3G**). Collectively, the above findings demonstrated that *A. indistinctus* was resistant to gastrointestinal juices and could be colonized in the intestine.

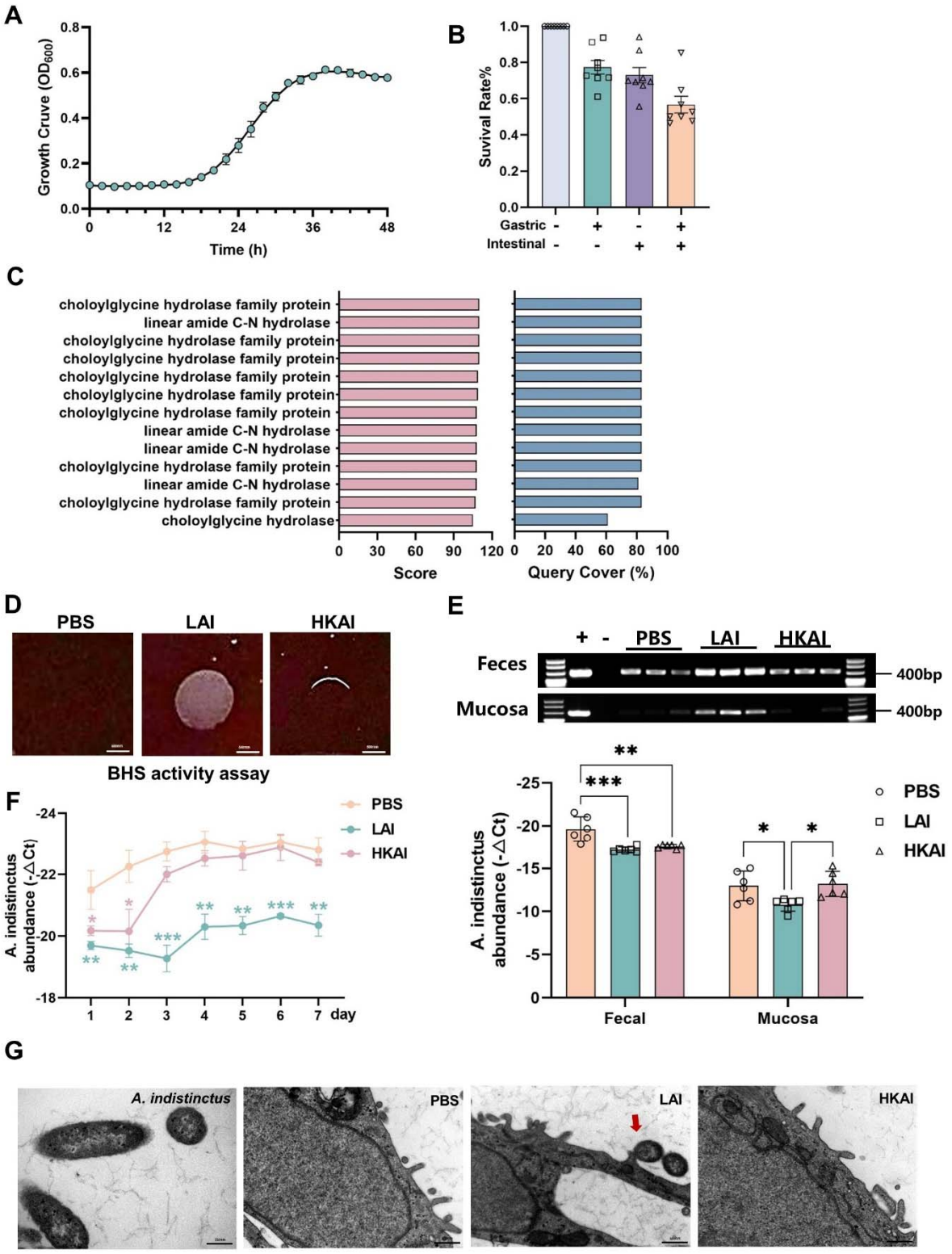

Figure 3. Gastrointestinal transit tolerance, BSH enzyme activity and colonization capacity of *A. indistinctus*. (A) Growth curve of *A. indistinctus*. (B) Survival rate of *A. indistinctus* in gastrointestinal digestion simulation. (C) Prediction of bile salt hydrolase activity of *A. indistinctus*. (D) Enzyme activity of bile salt hydrolase in *A. indistinctus*. (E) Quantification of *A. indistinctus* in feces and colon mucosa. (F) Relative abundance of *A. indistinctus* one week after the discontinuation of gavage. (G) Representative transmission electron microscope images of *A. indistinctus* (the red arrow) attaching to Caco-2 cells (Scale bars, 250 nm for *A. indistinctus*; 500 nm for the remaining panels). Data were presented as mean ± SEM (n=3 independent experiments for A, D and G, n=8 independent experiments for B, n=6 per group for E and F), and *P* values were determined by one-way ANOVA followed by Tukey's test. $^{*}P < 0.05$, $^{**}P < 0.01$, and $^{***}P < 0.001$.

3.3 A. indistinctus enhances intestinal barrier

3.3.1 A. indistinctus-mediated enhancement of intestinal barrier function in germ-free mice

Then, the effects of *A. indistinctus* on gut integrity, the defect of which contributed to a broad range of diseases[27], were further evaluated *in vivo* and *in vitro*. GF mice with impaired mucus secretion were firstly treated with both live and heat-killed *A. indistinctus* for 4 weeks to examine its ability to restore the first line of physical defense[28-30]. H&E and AB-PAS staining of colon sections demonstrated that only live *A. indistinctus* increased the number of goblet cells by 1.5-fold and enhanced mucus layer thickness by 2-fold (**Figure 4A**). Moreover, several mucus-related genes, including *muc2*, *zymogen granule protein 16* (*Zg16*) and *Fc gamma binding protein* (*fcgbp*), was found to be remarkably higher in mice gavaged with live *A. indistinctus*, which was absent in mice treated with pasteurized *A. indistinctus* (**Figure 4B**). Consistently, live but not heat-killed *A. indistinctus* supplementation led to a 1.5-fold increase in colonic MUC2 expression (**Figure 4C and 4D**), further suggesting that the enhanced MUC2 production depended on the viability of *A. idistinctus*. Additionally, an increasing trend in the expression of tight junction proteins at both the mRNA and protein levels were also found in GF mice gavaged with live *A. indistinctus* (**Figure S1A-S1C**), suggesting a protective effect on physical barrier.

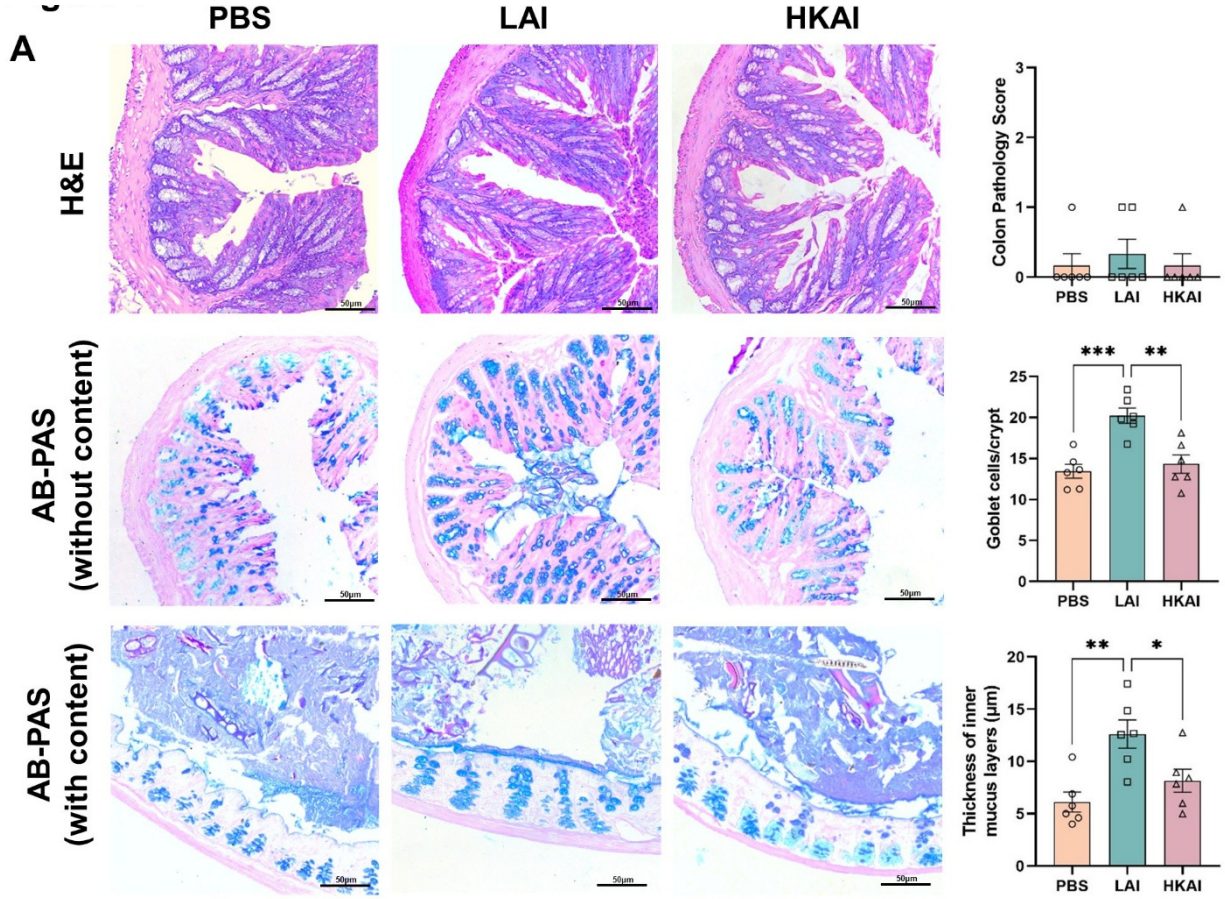

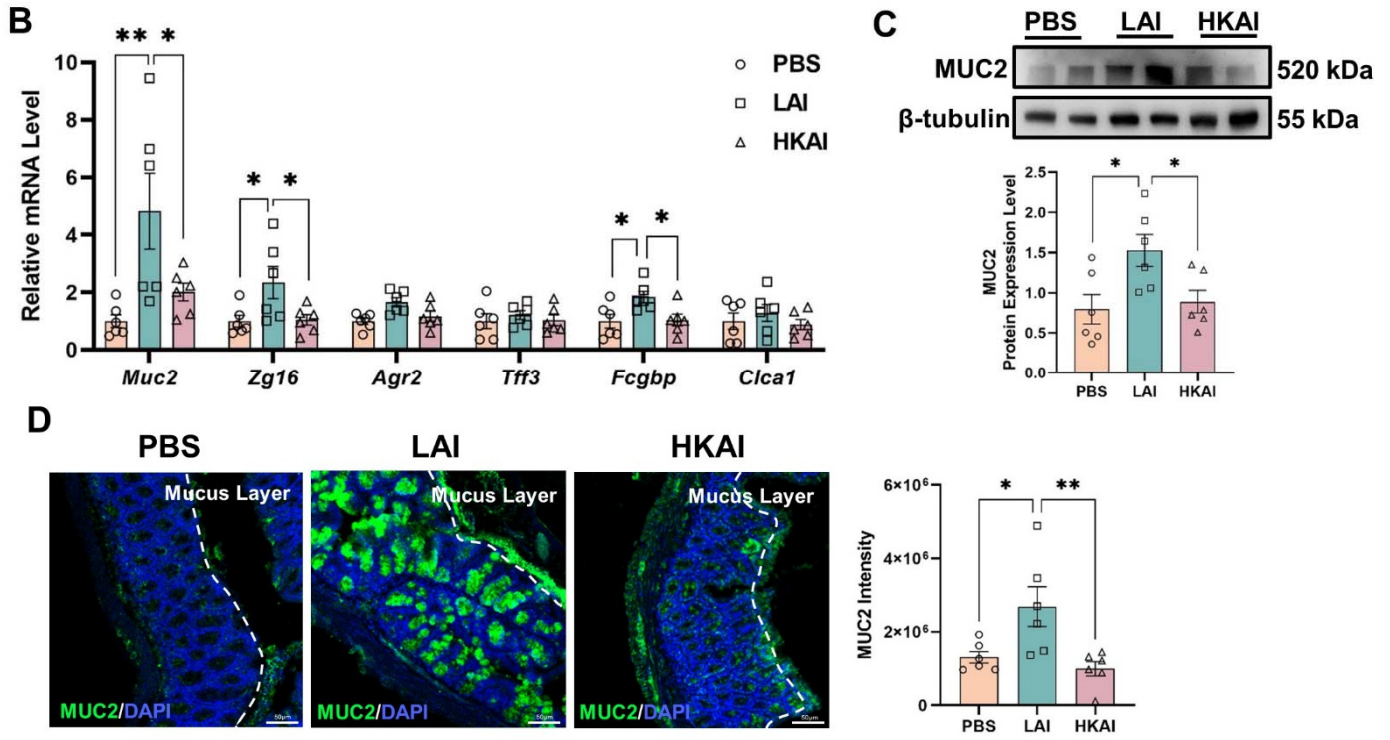

Figure 4. *A. indistinctus*-mediated enhancement of intestinal barrier function in germ-free mice. (A) Representative images of H&E and Periodic Acid Schiff-Alcian Blue staining in the colon (Scale bars, 50 μm). (B) Relative mRNA expression of mucin secretion-related genes in the colon. (C) Representative immunoblotting and quantification of MUC2 in the colon. (D) Representative immunofluorescence staining of mucus layer in the colon (Scale bars, 50 μm). Data were presented as mean ± SEM (n=6 per group) and *P* values were determined by one-way ANOVA followed by Tukey's test. $^{*}P < 0.05$, $^{**}P < 0.01$, and $^{***}P < 0.001$.

3.3.2 The promotion of MUC2 secretion and epithelial integrity by A. indistinctus in vitro

Moreover, LS174T cells were employed to evaluate the potential of *A. indistinctus* to promote mucin secretion in goblet cells. In cells challenged with LPS, *A. indistinctus* treatment enhanced the expression of MUC2 by 88.62%, reversing it to basal conditions. Consistently, immunofluorescence staining demonstrated that *A. indistinctus* effectively attenuated LPS-induced impairment in MUC2 production (**Figure 5B and 5C**). Subsequently, the potential of *A. indistinctus* to enhance intestinal epithelial barrier integrity was assessed in Caco-2 cells. Co-culture with *A. indistinctus* increased the TEER by 12.54% under basal conditions, and reversed LPS-induced epithelial injury by around 20% (**Figure 5D**). Similarly, *A. indistinctus* exposure substantially attenuated LPS-induced paracellular permeability, restoring it to basal conditions (**Figure 5E**). Compared to PBS control, LPS stimulation downregulated the expression of tight junctions, including *ZO-1*, zonula occludens-2 (*ZO-2*), *OCLN* and cingulin (*CGN*), by 35.17%. However, pretreatment with *A. indistinctus* prior to LPS exposure almost completely abolished the compromise in tight junctions induced by LPS and restored the expression of *ZO-1* and *OCLN* (**Figure 5F**). Consistently, LPS-induced reduction of ZO-1 and OCLN at protein level was readily reversed by *A. indistinctus* (**Figure 5G and 5H**).

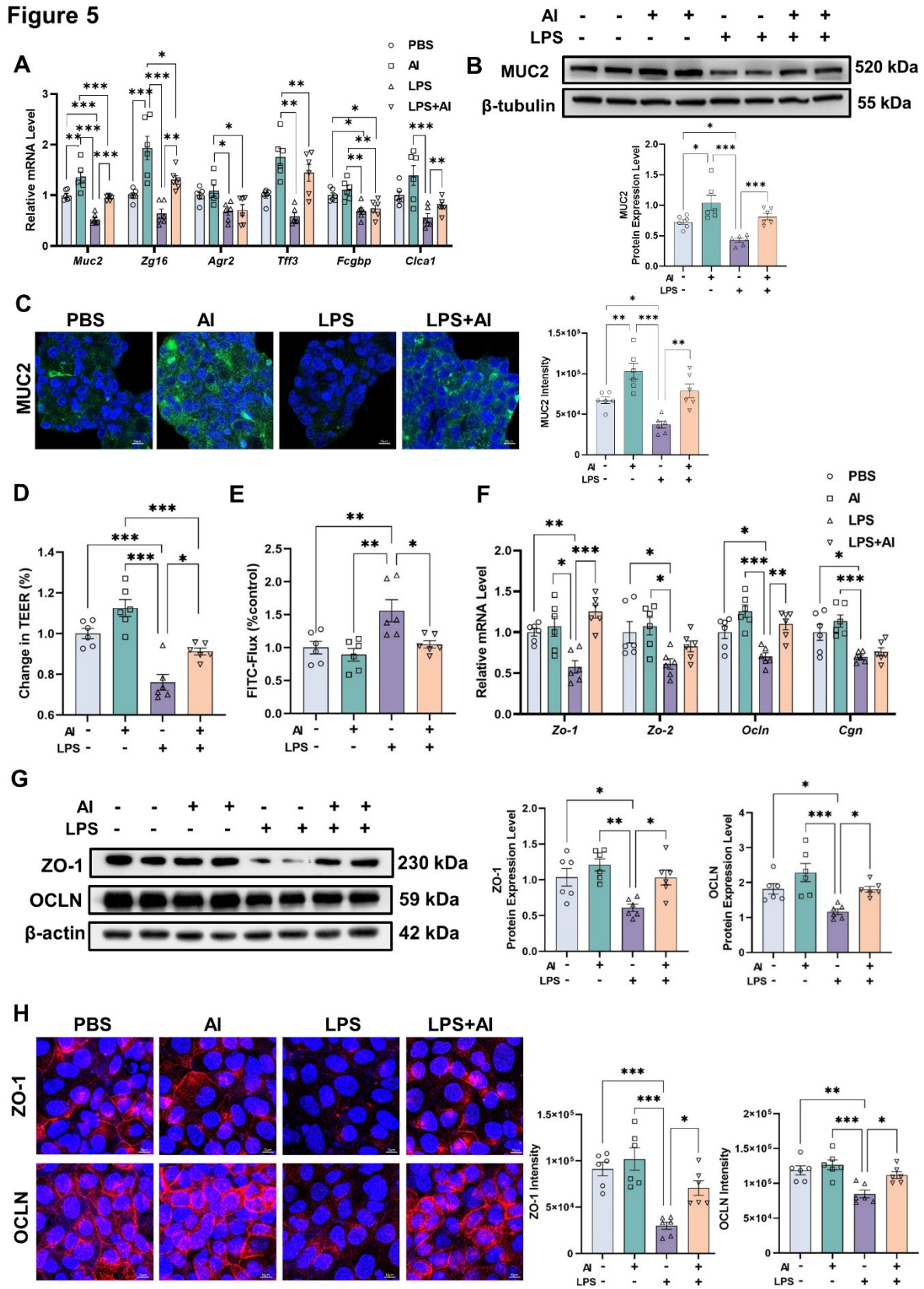

Figure 5. The promotion of MUC2 secretion and epithelial integrity by *A. indistinctus*. (A) Relative mRNA expression of mucin secretion-related genes in LS174T cells. (B) Representative immunoblotting and quantification of MUC2 in LS174T cells. (C) Representative immunofluorescence staining of MUC2 in LS174T cells (Scale bars, 10 μm). (D) Trans-epithelial electrical resistance value. (E) Fluorescein isothiocyanate flux. (F) Relative mRNA expression of *ZO-1*, *ZO-2*, *OCLN* and *CGN* in Caco-2 cells. (G) Representative immunoblotting and quantification of ZO-1 and OCLN in Caco-2 cells. (H) Representative immunofluorescence staining of ZO-1 and OCLN in Caco-2 cells (Scale bars, 10 μm). Data were presented as mean ± SEM (n=6 independent experiments), and *P* values were determined by one-way ANOVA followed by Tukey's test. $^{*}P < 0.05$, $^{**}P < 0.01$, and $^{***}P < 0.001$.

3.3.3 The anti-inflammatory effect of A. indistinctus through NF-κB

Given that nuclear factor kappa-B (NF-κB)-mediated inflammation signaling regulates both mucin production and tight junction expression[31, 32], we further explored the anti-inflammatory effects of *A. indistinctus* in LS174T and Caco-2 cells. Compared to PBS control, LPS stimulation markedly increased the transcription of pro-inflammatory markers, such as *TNF-α*, *IL-1β*, and *IL-6*, whereas *A. indistinctus* treatment reversed these pro-inflammatory markers to basal levels (**Figure 6A and 6F**). Consistently, the secretion of these pro-inflammatory cytokines was reduced by approximately 20% upon *A. indistinctus* exposure (**Figure 6B and 6G**), demonstrating a strong anti-inflammatory capacity. Moreover, co-culture of *A. indistinctus* substantially suppressed LPS-induced nuclear translocation of NF-κB p65, leading to 60% reduction in phosphorylated NF-κB p65 in the nucleus (**Figure 6C-E and 6H-J**). Additionally, the anti-inflammatory potential of *A. indistinctus* was further validated in RAW 264.7 cells. As expected, LPS stimulation resulted in a remarkable rise in nitric oxide (NO) and prostaglandin E2 (PGE2) production, whereas, pretreatment with *A. indistinctus* reduced NO release by 49.50% and PGE2 production by 21.22% (**Figure 6K and 6L**). Taken together, the above findings demonstrated that *A. indistinctus* enhanced mucus barrier function and epithelial integrity by suppressing NF-κB-mediated inflammation activation.

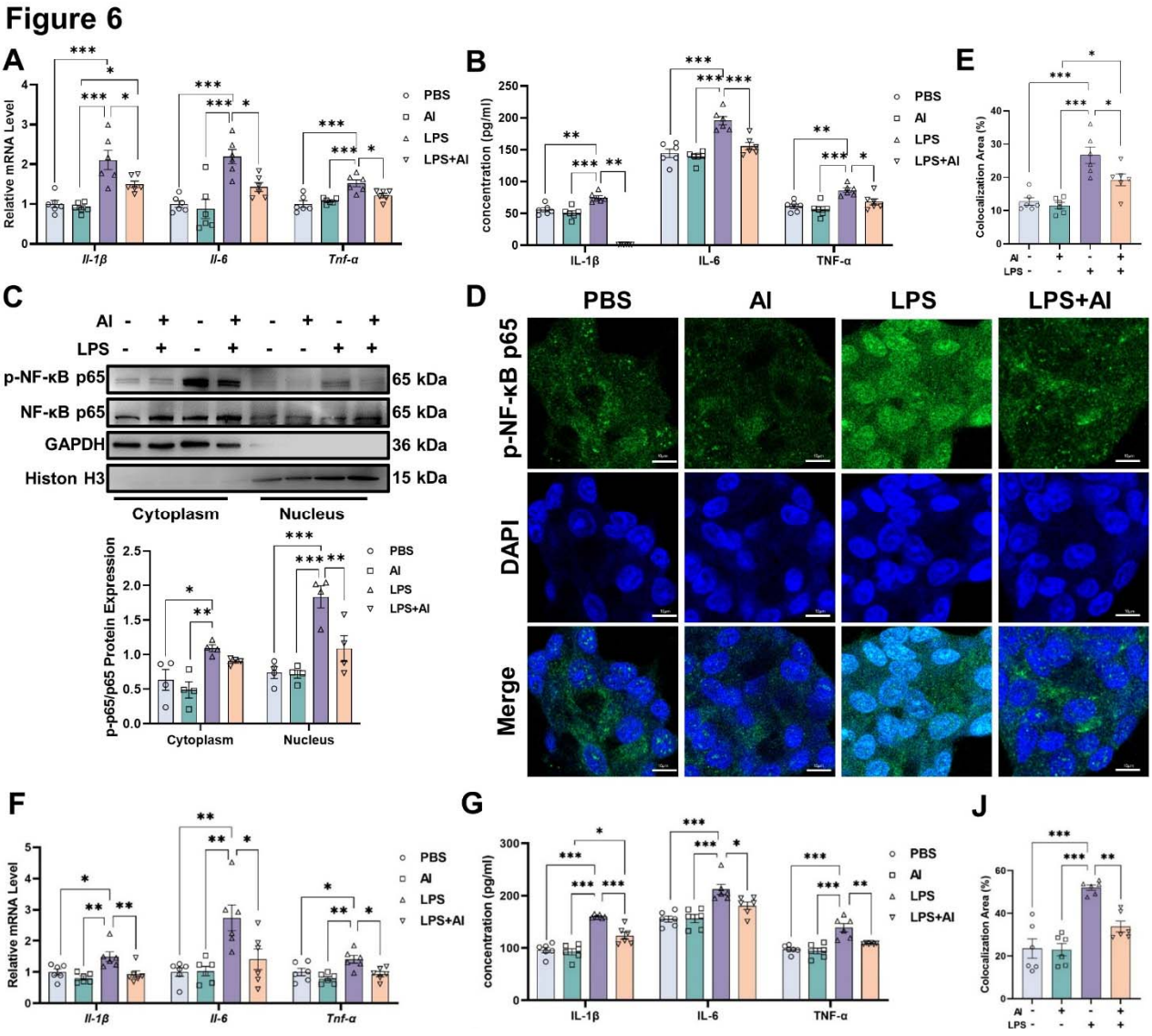

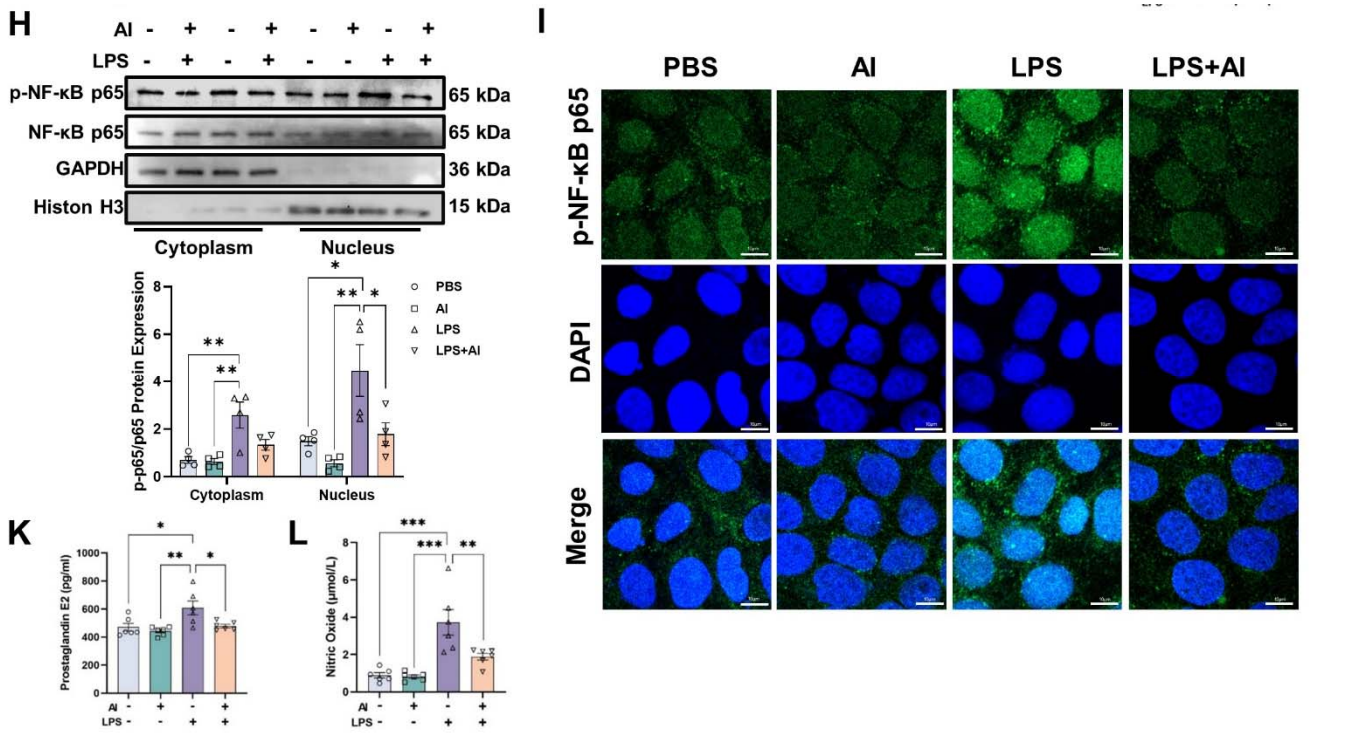

Figure 6. Anti-inflammatory effect of *A. indistinctus* via a suppression of NF-κB. (A-E) LS174T cells and (F-J) Caco-2 cells pretreated with *A. indistinctus* were exposed to LPS challenge for another 24h before analysis. Relative mRNA expression of *IL-1β*, *IL-6* and *TNF-α* in (A) LS174T cells and (F) Caco-2 cells, respectively. Quantitation of IL-1β, IL-6 and TNF-α in the supernatant of (B) LS174T cells and (G) Caco-2 cells, respectively. Representative immunoblotting and quantification of p-NF-κB p65 and NF-κB p65 in the cytoplasm and nucleus of (C) LS174T cells and (H) Caco-2 cells, respectively. Nucleus translocation of p-NF-κB p65 in (D-E) LS174T cells and (I-J) Caco-2 cells, respectively (Scale bars, 10 μm). Data were presented as mean ± SEM (n=4 or 6 independent experiments), and *P* values were determined by one-way ANOVA followed by Tukey's test. $^{*}P < 0.05$, $^{**}P < 0.01$, and $^{***}P < 0.001$.

4. Discussion

As a non-sporulating, non-motile, Gram-negative bacterial strain initially isolated from the feces of healthy Japanese males[8], several studies have demonstrated the metabolic benefits of *A. indistinctus*, however, its probiotic properties have never been systematically evaluated. In this study, we found that *A. indistinctus* exhibited a high genomic sequence similarity with *Bifidobacterium* spp.. Oral administration of *A. indistinctus* enhanced MUC2 production in goblet cells and tight junction proteins in epithelial cells. Mechanistically, *A. indistinctus* enhanced gut integrity and protected against LPS-induced inflammation by suppressing the nuclear translocation and activation of NF-κB. Additionally, with a strong resistance to gastric and intestinal juices, *A. indistinctus* demonstrated a high adherence capacity to intestinal villi, which facilitated its effective colonization.

Consistent with the comparative genomic analysis revealing a high similarity to *Bifidobacterium* spp., *A. indistinctus* showed comparable colonization capacity and probiotic properties with *Bifidobacterium* spp.. For example, similar to the observation that various species from *Bifidobacterium* spp., such as *Bifidobacterium longum*, *Bifidobacterium breve* and *Bifidobacterium dentium* (*B. dentium*), were able to ameliorate colonic inflammation through the enhancement of MUC2 protein secretion from goblet cell[30, 33, 34], administration of *A. indistinctus* led to a 1.5-fold increase in colonic MUC2 expression (**Figure. 4C**). Likewise, *Bifidobacterium. bifidum* FL228.1 and *Bifidobacterium. animalis subsp. Lactis F1-7* were found to inhibit the

expression of inflammatory cytokines in the intestinal tract and relieve intestinal inflammation, thereby suppressing the overproduction of osteoclasts[18]. Here, in this study, we demonstrated that the enhanced mucus barrier function and epithelial integrity induced by *A. indistinctus* was associated with its suppression of NF-κB nucleus translocation and activation (**Figure. 6C-6E and Figure. 6H-6J**), further suggesting that anti-inflammatory property is a common feature of probiotics. Moreover, similar to *B. dentium* N8, a strain with survivability in the simulated gastrointestinal conditions[19], *A. indistinctus* was able to encode a variety of genes related to the enzyme activity of BSH and exhibited a strong gastrointestinal tract tolerance (**Figure. 3B and 3C**), which in turn facilitated its colonization. Furthermore, consistent with the positive associations between *A. indistinctus* and metabolic health in diverse populations[10, 13, 35], *A. indistinctus* showed no cytotoxicity toward Caco-2 cells or histopathological damage in the liver and kidney in murine models (**Figure. 2A-2F**), supporting its safety as a probiotic supplementation. While its long-term safety warrants further investigation in various models, *A. indistinctus* represents a promising next-generation probiotic.

The intestine is the largest and one of the most important internal barriers in the body, which protects the host from noxious substance and microbes in the gut lumen[1]. Given its indispensable role in health, maintaining gut barrier integrity has been recognized as a key mechanism through which probiotics exert their beneficial effects[36]. Previous studies demonstrated that the majority of well-established probiotics, primarily from *Lactobacillus* spp. and *Bifidobacterium* spp., positively regulated tight junction gene expression, thereby enhancing barrier integrity and mitigating LPS-induced intestinal inflammation[37, 38]. Similarly, specific strains of *A. muciniphila*, *Faecalibacterium prausnitzii* (*F. prausnitzii*), *Bacteroides xylanisolvens*, *Bacteroides uniformis* and *Pediococcus acidilactici* had also been extensively studied for their role in intestinal integrity[39-43]. Specifically, *A. muciniphila* increased goblet cell numbers, normalized the thickness of mucus in the inner layer, and strengthened the intestinal mucus barrier[44], while *F. prausnitzii* enhanced tight junction gene expression and improved barrier function[45]. In a similar fashion, *A. indistinctus* suppressed NF-κB-mediated inflammatory signaling activation, thereby promoting the restoration of intestinal integrity. Given that impaired gut integrity is a shared pathological feature of metabolic disorders[46], like type 2 diabetes and metabolic dysfunction-associated fatty liver disease, the ability of *A. indistinctus* to ameliorate glucose intolerance and hepatic lipid accumulation may also attributable to its reinforcement of the gut barrier. Though *A. indistinctus* had been proved to be effective and safe at a dose of 5×10^8 cfu/day, more studies with various dosages and longer durations are warranted to further evaluate its safety. Moreover, the microbial effectors conferring its beneficial effect on gut integrity remain elusive. Given its central role in the microbial community[47], *A. indistinctus* may promote the growth of other beneficial species, such as *Lactobacillus johnsonii*, and *Blautia* spp., and act in concert to main the integrity of intestinal barrier. Additionally, considering that metabolites and secretory proteins function as common effectors of next-generation probiotics, such as *F. prausnitzii* and *A. muciniphila*[48, 49], *A. indistinctus* may also exert its protective effect via bioactive molecules. Future studies integrated with multi-omics are warranted to figure out the bioactive molecules conferring the intestinal barrier repair effect of *A. indistinctus*.

The ability to adhere to and colonize in host intestine mucosa both during and after supplementation[50], which facilitates the interaction between the host and microorganism, is an indispensable prerequisite for probiotics to exert their beneficial effects. Consistent with the genomic analysis that *A. indistinctus* encoded *tuf* gene (**Figure 1A**), a mucus binding protein associated with adhesion and colonization[20], live *A. indistinctus* was able to colonize the intestinal mucosa and persisted in the intestine for at least one week after supplementation ceased (**Figure. 3F**). In contrast, the heat-killed *A. indistinctus* failed to colonize the intestinal mucus, suggesting that the adhesion protein was heat sensitive. Consistently, significant uric acid-lowering effect was exclusively observed in live *A. indistinctus*[13], further underscoring the importance of adhesion capability in the probiotic properties of *A. indistinctus*. Similarly, only live *B. dentium* was reported to be able to colonize in the ileal mucus layer and influenced adult behaviors via its metabolite acetate, whereas minimal heat-killed *B. dentium* was detected in the colon, as confirmed by fluorescence *in situ* hybridization[51]. Another key probiotic characteristic is survival in the harsh gastrointestinal environment[52]. Although previous studies suggested that *A. indistinctus* was sensitive to 20% bile acid[8], we found that aligned with its ability to encode BSH enzymes which deconjugated glycine or taurine from the steroid core[53], *A. indistinctus* demonstrated a strong gastrointestinal tolerance (**Figure. 3B**), comparable to *Bifidobacterium* spp. and *Lactobacillus* spp., lending further support to its potential as an oral probiotic[19, 54]. Although influenced by various factors, such as host immune status, gut motility, and resident microbiota composition[55], *A. indistinctus* was prevalent in the general population, with an average colonization rate ranging from 52% to 69%[9]. To further evaluate the colonization capacity of *A. indistinctus*, more research in diverse populations is warranted.

5. Conclusion

In summary, our results demonstrates that *A. indistinctus* holds promise as a next-generation probiotic. Although more studies are warranted to further evaluate its safety and efficacy, especially in human clinical trials, and its synergetic effects with resident microbes, we believe that the identification of *A. indistinctus* as a next-generation probiotic is attractive in the field of probiotics-based functional foods.

Acknowledgements

This work was supported by the Natural Science Foundation of China (824B2098), Natural Science Foundation of Guangdong Province (2024A1515013226, 2023HYSPT0710), and the Fundamental Research Funds for the Central Universities (Sun Yat-sen University, 2025QNPY01).

Conflict of interest

The authors declare no competing financial interest.

References

[1] J.R. Turner, Intestinal mucosal barrier function in health and disease, Nat Rev Immunol. 9 (2009) 799-809. https://doi.org/10.1038/nri2653.

[2] M.E. Johansson, H. Sjövall, G.C. Hansson, The gastrointestinal mucus system in health and disease, Nat Rev Gastroenterol Hepatol. 10 (2013) 352-361. https://doi.org/10.1038/nrgastro.2013.35.

[3] C. Song, Z. Chai, S. Chen, et al., Intestinal mucus components and secretion mechanisms: what we do and do not know, Exp Mol Med. 55 (2023) 681-691. https://doi.org/10.1038/s12276-023-00960-y.

[4] L.W. Peterson, D. Artis, Intestinal epithelial cells: regulators of barrier function and immune homeostasis, Nat Rev Immunol. 14 (2014) 141-153. https://doi.org/10.1038/nri3608.

[5] C. Chelakkot, J. Ghim, S.H. Ryu, Mechanisms regulating intestinal barrier integrity and its pathological implications, Exp Mol Med. 50 (2018) 1-9. https://doi.org/10.1038/s12276-018-0126-x.

[6] L. Li, Y.J. Jiang, X.Y. Yang, et al., Immunoregulatory effects on Caco-2 cells and mice of exopolysaccharides isolated from Lactobacillus acidophilus NCFM, Food Funct. 5 (2014) 3261-3268. https://doi.org/10.1039/c4fo00565a.

[7] N. Shi, N. Li, X. Duan, et al., Interaction between the gut microbiome and mucosal immune system, Mil Med Res. 4 (2017) 14. https://doi.org/10.1186/s40779-017-0122-9.

[8] F. Nagai, M. Morotomi, Y. Watanabe, et al., Alistipes indistinctus sp. nov. and Odoribacter laneus sp. nov., common members of the human intestinal microbiota isolated from faeces, Int J Syst Evol Microbiol. 60 (2010) 1296-1302. https://doi.org/10.1099/ijs.0.014571-0.

[9] R. Gacesa, A. Kurilshikov, A. Vich Vila, et al., Environmental factors shaping the gut microbiome in a Dutch population, Nature. 604 (2022) 732-739. https://doi.org/10.1038/s41586-022-04567-7.

[10] D. Wu, L. Liu, N. Jiao, et al., Targeting keystone species helps restore the dysbiosis of butyrate-producing bacteria in nonalcoholic fatty liver disease, Imeta. 1 (2022) e61. https://doi.org/10.1002/imt2.61.

[11] J. Zheng, Q. Sun, M. Zhang, et al., Noninvasive, microbiome-based diagnosis of inflammatory bowel disease, Nat Med. 30 (2024) 3555-3567. https://doi.org/10.1038/s41591-024-03280-4.

[12] T. Takeuchi, T. Kubota, Y. Nakanishi, et al., Gut microbial carbohydrate metabolism contributes to insulin resistance, Nature. 621 (2023) 389-395. https://doi.org/10.1038/s41586-023-06466-x.

[13] Y.X. Xu, L.D. Liu, J.Y. Zhu, et al., Alistipes indistinctus-derived hippuric acid promotes intestinal urate excretion to alleviate hyperuricemia, Cell Host Microbe. 32 (2024) 366-381.e369. https://doi.org/10.1016/j.chom.2024.02.001.

[14] S. Salminen, M.C. Collado, A. Endo, et al., The International Scientific Association of Probiotics and Prebiotics (ISAPP) consensus statement on the definition and scope of postbiotics, Nat Rev Gastroenterol Hepatol. 18 (2021) 649-667. https://doi.org/10.1038/s41575-021-00440-6.

[15] S. Luo, Y. Zhao, S. Zhu, et al., Flavonifractor plautii Protects Against Elevated Arterial Stiffness, Circ Res. 132 (2023) 167-181. https://doi.org/10.1161/circresaha.122.321975.

[16] H. Plovier, A. Everard, C. Druart, et al., A purified membrane protein from Akkermansia muciniphila or the pasteurized bacterium improves metabolism in obese and diabetic mice, Nat Med. 23 (2017) 107-113. https://doi.org/10.1038/nm.4236.

[17] T. Streidl, I. Karkossa, R.R. Segura Muñoz, et al., The gut bacterium Extibacter muris produces secondary bile acids and influences liver physiology in gnotobiotic mice, Gut Microbes. 13 (2021) 1-21. https://doi.org/10.1080/19490976.2020.1854008.

[18] J. Zhang, X. Liang, X. Tian, et al., Bifidobacterium improves oestrogen-deficiency-induced osteoporosis in mice by modulating intestinal immunity, Food Funct. 15 (2024) 1840-1851. https://doi.org/10.1039/d3fo05212e.

[19] L. Zhao, Q. Xie, S. Etareri Evivie, et al., Bifidobacterium dentium N8 with potential probiotic characteristics prevents LPS-induced intestinal barrier injury by alleviating the inflammatory response and regulating the tight junction in Caco-2 cell monolayers, Food Funct. 12 (2021) 7171-7184. https://doi.org/10.1039/d1fo01164b.

[20] Y. Du, H. Li, W. Xu, et al., Cell surface-associated protein elongation factor Tu interacts with fibronectin mediating the adhesion of Lactobacillus plantarum HC-2 to Penaeus vannamei intestinal epithelium and inhibiting the apoptosis induced by LPS and pathogen in Caco-2 cells, Int J Biol Macromol. 224 (2023) 32-47. https://doi.org/10.1016/j.ijbiomac.2022.11.252.

[21] K. Al-Nedawi, M.F. Mian, N. Hossain, et al., Gut commensal microvesicles reproduce parent bacterial signals to host immune and enteric nervous systems, Faseb j. 29 (2015) 684-695. https://doi.org/10.1096/fj.14-259721.

[22] M.L. Van Tassell, M.J. Miller, Lactobacillus adhesion to mucus, Nutrients. 3 (2011) 613-636. https://doi.org/10.3390/nu3050613.

[23] N. Juge, Microbial adhesins to gastrointestinal mucus, Trends Microbiol. 20 (2012) 30-39. https://doi.org/10.1016/j.tim.2011.10.001.

[24] A.Y. Bustos, G. Font de Valdez, S. Fadda, et al., New insights into bacterial bile resistance mechanisms: the role of bile salt hydrolase and its impact on human health, Food Res Int. 112 (2018) 250-262. https://doi.org/10.1016/j.foodres.2018.06.035.

[25] Y. Liu, H. Duan, Y. Chen, et al., Intraspecific difference of Latilactobacillus sakei in inflammatory bowel diseases: Insights into potential mechanisms through comparative genomics and metabolomics analyses, Imeta. 2 (2023) e136. https://doi.org/10.1002/imt2.136.

[26] B. Rimal, S.L. Collins, C.E. Tanes, et al., Bile salt hydrolase catalyses formation of amine-conjugated bile acids, Nature. 626 (2024) 859-863. https://doi.org/10.1038/s41586-023-06990-w.

[27] H. Kayama, R. Okumura, K. Takeda, Interaction Between the Microbiota, Epithelia, and Immune Cells in the Intestine, Annu Rev Immunol. 38 (2020) 23-48. https://doi.org/10.1146/annurev-immunol-070119-115104.

[28] M.S. Desai, A.M. Seekatz, N.M. Koropatkin, et al., A Dietary Fiber-Deprived Gut Microbiota Degrades the Colonic Mucus Barrier and Enhances Pathogen Susceptibility, Cell. 167 (2016) 1339-1353.e1321. https://doi.org/10.1016/j.cell.2016.10.043.

[29] M.E. Johansson, H.E. Jakobsson, J. Holmén-Larsson, et al., Normalization of Host Intestinal Mucus Layers Requires Long-Term Microbial Colonization, Cell Host Microbe. 18 (2015) 582-592. https://doi.org/10.1016/j.chom.2015.10.007.

[30] B.O. Schroeder, G.M.H. Birchenough, M. Ståhlman, et al., Bifidobacteria or Fiber Protects against Diet-Induced Microbiota-Mediated Colonic Mucus Deterioration, Cell Host Microbe. 23 (2018) 27-40.e27. https://doi.org/10.1016/j.chom.2017.11.004.

[31] X. Chen, J. Wu, X. Fu, et al., Fructus mori polysaccharide alleviates diabetic symptoms by regulating intestinal microbiota and intestinal barrier against TLR4/NF-κB pathway, Int J Biol Macromol. 249 (2023) 126038. https://doi.org/10.1016/j.ijbiomac.2023.126038.

[32] J. Bai, S. Deng, X. Zhang, et al., Cinnamaldehyde alleviates zearalenone-induced LS174T cell apoptosis, barrier dysfunction and mucin reduction through JNK/NF-κB signaling pathway, Ecotoxicol Environ Saf. 263 (2023) 115276. https://doi.org/10.1016/j.ecoenv.2023.115276.

[33] Y. Li, H. Xu, L. Zhou, et al., Bifidobacterium breve Protects the Intestinal Epithelium and Mitigates Inflammation in Colitis via Regulating the Gut Microbiota-Cholic Acid Pathway, J Agric Food Chem. 72 (2024) 3572-3583. https://doi.org/10.1021/acs.jafc.3c08527.

[34] M.A. Engevik, B. Herrmann, W. Ruan, et al., Bifidobacterium dentium-derived y-glutamylcysteine suppresses ER-mediated goblet cell stress and reduces TNBS-driven colonic inflammation, Gut Microbes. 13 (2021) 1-21. https://doi.org/10.1080/19490976.2021.1902717.

[35] B.J. Parker, P.A. Wearsch, A.C.M. Veloo, et al., The Genus Alistipes: Gut Bacteria With Emerging Implications to Inflammation, Cancer, and Mental Health, Front Immunol. 11 (2020) 906. https://doi.org/10.3389/fimmu.2020.00906.

[36] Y. Zheng, Z. Zhang, P. Tang, et al., Probiotics fortify intestinal barrier function: a systematic review and meta-analysis of randomized trials, Front Immunol. 14 (2023) 1143548. https://doi.org/10.3389/fimmu.2023.1143548.

[37] A.B. Shah, A. Baiseitova, M. Zahoor, et al., Probiotic significance of Lactobacillus strains: a comprehensive review on health impacts, research gaps, and future prospects, Gut Microbes. 16 (2024) 2431643. https://doi.org/10.1080/19490976.2024.2431643.

[38] S.J. Gavzy, A. Kensiski, Z.L. Lee, et al., Bifidobacterium mechanisms of immune modulation and tolerance, Gut Microbes. 15 (2023) 2291164. https://doi.org/10.1080/19490976.2023.2291164.

[39] P.D. Cani, W.M. de Vos, Next-Generation Beneficial Microbes: The Case of Akkermansia muciniphila, Front Microbiol. 8 (2017) 1765. https://doi.org/10.3389/fmicb.2017.01765.

[40] R. Martín, S. Miquel, L. Benevides, et al., Functional Characterization of Novel Faecalibacterium prausnitzii Strains Isolated from Healthy Volunteers: A Step Forward in the Use of F. prausnitzii as a Next-Generation Probiotic, Front Microbiol. 8 (2017) 1226. https://doi.org/10.3389/fmicb.2017.01226.

[41] T. Fu, Y. Wang, M. Ma, et al., Isolation of Alginate-Degrading Bacteria from the Human Gut Microbiota and Discovery of Bacteroides xylanisolvens AY11-1 as a Novel Anti-Colitis Probiotic Bacterium, Nutrients. 15 (2023) https://doi.org/10.3390/nu15061352.

[42] S. Zhang, Q. Nie, Y. Sun, et al., Bacteroides uniformis degrades β-glucan to promote Lactobacillus johnsonii improving indole-3-lactic acid levels in alleviating colitis, Microbiome. 12 (2024) 177. https://doi.org/10.1186/s40168-024-01896-9.

[43] I.K. Woo, J.H. Hyun, H.J. Jang, et al., Probiotic Pediococcus acidilactici Strains Exert Anti-inflammatory Effects by Regulating Intracellular Signaling Pathways in LPS-Induced RAW 264.7 Cells, Probiotics Antimicrob Proteins. (2024) https://doi.org/10.1007/s12602-024-10263-x.

[44] Q. Nie, X. Luo, K. Wang, et al., Gut symbionts alleviate MASH through a secondary bile acid biosynthetic pathway, Cell. 187 (2024) 2717-2734.e2733. https://doi.org/10.1016/j.cell.2024.03.034.

[45] X. Wang, Y. Li, X. Wang, et al., Faecalibacterium prausnitzii Supplementation Prevents Intestinal Barrier Injury and Gut Microflora Dysbiosis Induced by Sleep Deprivation, Nutrients. 16 (2024) https://doi.org/10.3390/nu16081100.

[46] J. Martel, S.H. Chang, Y.F. Ko, et al., Gut barrier disruption and chronic disease, Trends Endocrinol Metab. 33 (2022) 247-265. https://doi.org/10.1016/j.tem.2022.01.002.

[47] X. Xu, Y. Wang, X. Wu, et al., Administration of Alistipes indistinctus prevented the progression from nonalcoholic fatty liver disease to nonalcoholic steatohepatitis by enhancing the gut barrier and increasing Lactobacillus spp, Biochem Biophys Res Commun. 741 (2024) 151033. https://doi.org/10.1016/j.bbrc.2024.151033.

[48] E. Quévrain, M.A. Maubert, C. Michon, et al., Identification of an anti-inflammatory protein from Faecalibacterium prausnitzii, a commensal bacterium deficient in Crohn's disease, Gut. 65 (2016) 415-425. https://doi.org/10.1136/gutjnl-2014-307649.

[49] S. Xie, J. Li, F. Lyu, et al., Novel tripeptide RKH derived from Akkermansia muciniphila protects against lethal sepsis, Gut. 73 (2023) 78-91. https://doi.org/10.1136/gutjnl-2023-329996.

[50] J. Suez, N. Zmora, E. Segal, et al., The pros, cons, and many unknowns of probiotics, Nat Med. 25 (2019) 716-729. https://doi.org/10.1038/s41591-019-0439-x.

[51] M.A. Engevik, B. Luck, C. Visuthranukul, et al., Human-Derived Bifidobacterium dentium Modulates the Mammalian Serotonergic System and Gut-Brain Axis, Cell Mol Gastroenterol Hepatol. 11 (2021) 221-248. https://doi.org/10.1016/j.jcmgh.2020.08.002.

[52] H. Rabah, F.L. Rosa do Carmo, G. Jan, Dairy Propionibacteria: Versatile Probiotics, Microorganisms. 5 (2017) https://doi.org/10.3390/microorganisms5020024.

[53] M. Begley, C. Hill, C.G. Gahan, Bile salt hydrolase activity in probiotics, Appl Environ Microbiol. 72 (2006) 1729-1738. https://doi.org/10.1128/aem.72.3.1729-1738.2006.

[54] X. Li, D. Hu, Y. Tian, et al., Protective effects of a novel Lactobacillus rhamnosus strain with probiotic characteristics against lipopolysaccharide-induced intestinal inflammation in vitro and in vivo, Food Funct. 11 (2020) 5799-5814. https://doi.org/10.1039/d0fo00308e.

[55] J. Wilde, E. Slack, K.R. Foster, Host control of the microbiome: Mechanisms, evolution, and disease, Science. 385 (2024) eadi3338. https://doi.org/10.1126/science.adi3338.